JJEE
Volume 6, Number 2, 2020
Pages 168-178
Jordan Journal of Electrical Engineering
ISSN (Print): 2409-9600, ISSN (Online): 2409-9619

COVID-19 Detection from X-ray Images Using Different Artificial Intelligence Hybrid Models

Ali Mohammad Alqudah[1*], Shoroq Qazan[2], Hiam Alquran[1], Isam Abu Qasmieh[1] Amin Alqudah[2]

[1] Department of Biomedical Systems and Informatics Engineering, Yarmouk University, Irbid, Jordan
E-mail: ali_qudah@hotmail.com
[2] Department of Computer Engineering, Yarmouk University, Irbid, Jordan

Received: March 27, 2020 *Revised: April 25, 2020* *Accepted: May 05, 2020*

***Abstract*—** COVID-19 leads to severe respiratory symptoms that are associated with highly intensive care unit (ICU) admissions and deaths. Early diagnosis of coronavirus limits its wide spread. Real-time reverse transcription-polymerase chain reaction (RT-PCR) is the strategy that has been used by clinicians to discover the presence or absence of this type of virus. This technique has a relatively low positive rate in the early stage of this disease. Therefore, clinicians call for other ways to help in the diagnosis of COVID-19. The appearance of X-ray chest images in case of COVID-19 is different from any other type of pneumonic disease. Therefore, this research is devoted to employ artificial intelligence techniques in the early detection stages of COVID-19 from chest X-ray images. Different hybrid models – each consists of deep features extraction and classification techniques - are implemented to assist clinicians in the detection of COVID-19. Convolutional neural network (CNN) is used to extract the graphical features in the implementations of the hybrid models from the chest X-ray images. The classification, to COVID-19 or Non-COVID-19, is achieved using different machine learning algorithms such as CNN, support vector machine (SVM), and random forest (RF), to obtain the best recognition performance. The most significant two extracted features are employed for training and parameters testing. According to the performance results of the designed models, CNN outperforms other classifiers with a testing accuracy of 95.2%.

***Keywords*—** COVID-19; Chest X-ray images; Convolutional neural network; Support vector machine, Random forest; Deep learning; Machine learning; Artificial intelligence.

1. INTRODUCTION

The most recent type of coronavirus that was first identified in Wuhan, Hubei Province is COVID-19. This novel coronavirus was initially reported in viral pneumonia cases. It is spreading worldwide and considered as a pandemic disease. The dramatic increase in the number of infected cases around the world leads the World Health Organization to name it as 2019-nCoV [1]. This novel coronavirus causes severe acute respiratory syndrome and is now formally named as SARS-CoV-2 [2]. Feng Pan et al. used chest computed tomography (CT) to assess the severity of lung damage in COVID-19 pneumonic, and concluded that the CT-chest images of the recovering COVID-19 patients showed lung disease severity after 10 days of the initial symptoms [3]. Rabi, Firas A., et al. presented a summary of all current issues regarding the novel coronavirus and the symptoms it causes from a medical point of view [4].

Quarantine and appropriate treatment for suspected cases are the most suitable methods to control the spreading of coronavirus. The pathogenic laboratory test is used as a diagnostic tool for coronavirus suspected cases, but it is time-consuming and has a significant false negative rate. In the early stage detection of COVID-19, some patients may have positive pulmonary imaging manifestations, but they may have no sputum findings and therefore, have negative test results in swabs of real-time reverse transcription-polymerase chain reaction (RT-PCR). These cases are not diagnosed as suspected or confirmed cases [5, 6].

* Corresponding author
Article's DOI: 10.5455/jjee.204-1585312246

In [7], a method was proposed for detecting coronavirus based on image processing techniques by measuring the fringe shift concerning the background. The authors obtained higher contrast images using multiple-beams rather than just two beams interference. The refractive index of the coronavirus is concluded from the fringe shift. In [5], deep learning algorithms were employed in classifying CT images of 618 subjects into three categories: COVID-19, influenza A, and healthy persons. The authors obtained an accuracy of 86.7%. In [6], the researchers used deep learning techniques as well to extract graphical features from CT images, and supply the clinician pre-diagnosis before the pathogenic test. They achieved 89.5% accuracy and 87% sensitivity, but the accuracy of their algorithm was 79.3% when it is applied to external dataset.

This hot topic has motivated many researchers to find an accurate diagnostic tool to limit COVID-19 outbreak. All the previous relevant studies have discussed this topic from a medical point of view, and others utilized the manifestations of pulmonary CT images using deep learning in classifying the COVID-19 cases. In this paper, we employ machine learning techniques in classifying and extracting graphical features from chest X-ray images of COVID-19 and Non-COVID-19 cases automatically, and finally comparing between different classifiers to identify the best candidate among all.

2. HYBRID MODELS ARCHITECTURES

In this section, we will describe the proposed models used in detecting COVID-19 from chest X-ray images. The proposed hybrid models share the feature extraction technique and vary in the classification techniques. The architecture consists of the following six modules: dataset preparation, convolutional neural network (CNN) training, graphical features extraction, classification using Softmax classifier, classification using SVM classifiers, and classification using RF classifier. Fig. 1 below shows the block diagram of the proposed hybrid models.

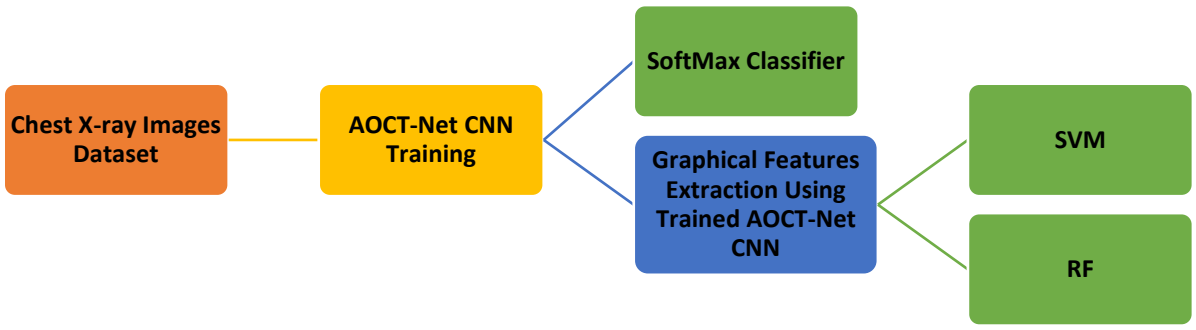

Fig. 1. Block diagram of the proposed hybrid models.

2.1. Dataset Preparation

The used dataset is the first worldwide publicly available database of COVID-19 cases with chest X-ray or CT images, in addition to cases from Middle East respiratory syndrome (MERS), severe acute respiratory syndrome (SARS), and acute respiratory distress syndrome

(ARDS). All images are 8-bit gray level with a size of 128 x 128, and data are released and publicly available [8]. Currently, the dataset only contains 71 chest X-ray images (48 cases for COVID-19 and 23 for Non-COVID-19). The dataset was created by collecting images from publications and making them available for research purposes [9]. This dataset also has been augmented and published online by Alqudah and Qazan [10]. The augmentation has been done to prevent the CNN from overfitting the training images dataset. The augmentation includes several geometric image transformations, namely, flipping, rotation, translation and scaling. As a consequence, the total number of images increased from 48 of each class to 912 which makes the dataset more appropriate for deep learning training [10, 11]. 18 operations have been deployed on each of the 48 images. They include Y-axis flipping, X-axis flipping, rotating with random degree, image scaling with a factor of 2, and image scaling of a factor of 0.5 [11]. In this work, we used the original dataset proposed by Joseph Cohen with the augmentation suggested here including a random number along both x and y axes (-5, 5) as well as random rotation (0^o - 360^o), and a random scaling (0.5 - 1). Fig. 2 shows X-ray images from the original dataset for Non-COVID-19 and COVID-19 subjects, respectively.

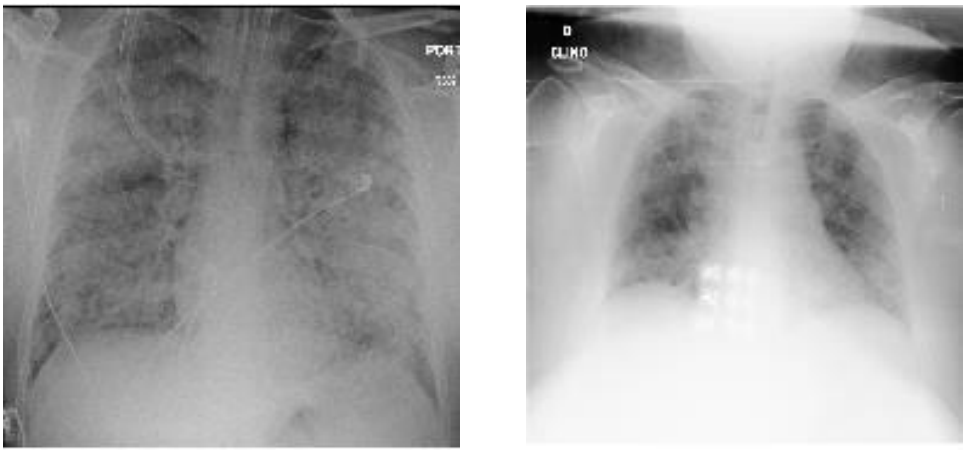

(a) (b)

Fig. 2. Image samples in the used dataset: a) Non-COVID-19; b) COVID-19 [8].

2.2. CNN training and Softmax Classification

This step aims to retrain the advanced optical coherence tomography network (AOCT-Net) on chest X-ray images using the transfer learning technique; then, using this trained AOCT-Net to extract deep features from the fully connected (FC) layer. CNN is a type of traditional artificial neural network (ANN), which is composed of neurons that own learnable weights alongside biases. It is composed from convolutional layers, pooling layers, rectified linear unit (ReLU) layers, and it is ended by FC layer. An input image pixel is entered for every neuron, followed by the calculation of a dot product and the elective non-linearity capture [12]. The input layer represents an image with enhancement such as mean subtraction and feature-scaling. The most distinguished feature of CNNs over ANNs is the huge numbers of hidden layers that are comprised of convolution layers, consisting of a set of learnable filters to identify predictive features in the input image.

The spatial coordinate of the feature map is reduced by pooling layers. This is performed by applying a window on the image with specific stride shifting across all the input pixels. There is another method which is based on the average value and it can be

applied in the pooling layer. ReLU layer introduces the nonlinearity of the network with its function f(x) = max (0, x) [11]. The last layer in all CNN models is the FC layer. This layer precedes the softmax and classification layers. The output of this layer represents the deep features that have been extracted and which are used for classification in the proceeding layers. The results are generated as a matrix where the columns represent the number of classes and the rows represent the number of the images [13].

The AOCT-Net is employed in this paper to classify the chest X-ray images [14]. It is started by the first convolutional layer that uses 32 filters with a size of 3×3 and one padding zeros, whereas rest of the convolutional layers utilize 16 filters of the same size, except for the third layer that uses only 8 filters. In order to decrease the time consumption, accelerate the training stage and decrease the sensitivity of the network initialization, the batch normalization layer is added between the convolutional layer and the nonlinearity layer (ReLU). Max pooling layer is utilized in AOCT-Net with a window size of 2×2 and increments 2 pixels as well. The output layer consists of FC layer with output size of 2, Softmax layer, and a classification layer. Fig. 3 illustrates the graphical representation of the AOCT-Net.

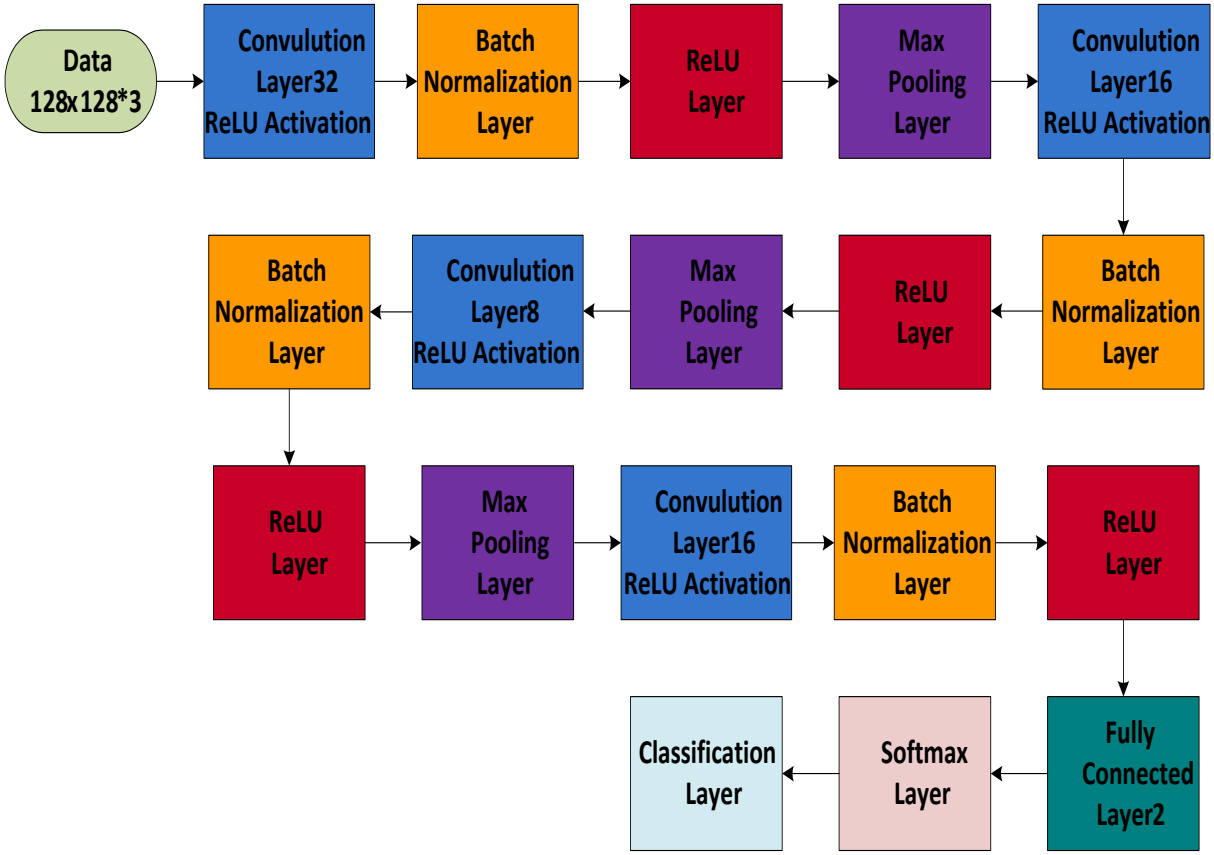

Fig. 3. Graphical representation of the AOCT-Net layers.

2.3. Features Extraction

The automated graphical features are extracted from the FC layer of the AOCT-NET. One feature is extracted from the COVID-19 cases and the other from Non-COVID-19. The scatter distribution of these two features is represented in Fig. 4. These scatter plots show the values of the extracted features for the training, testing, and the whole dataset. From these features, we can notice that the used CNN architecture succeeds in extracting features that

are able to distinguish between the two classes (COVID-19 and Non-COVID-19). The time required for extracting the features from the FC layer in the training stage for the whole dataset is 2.26 s. These extracted features are exploited to build classifying models using support vector machine (SVM) and random forest (RF) classifiers.

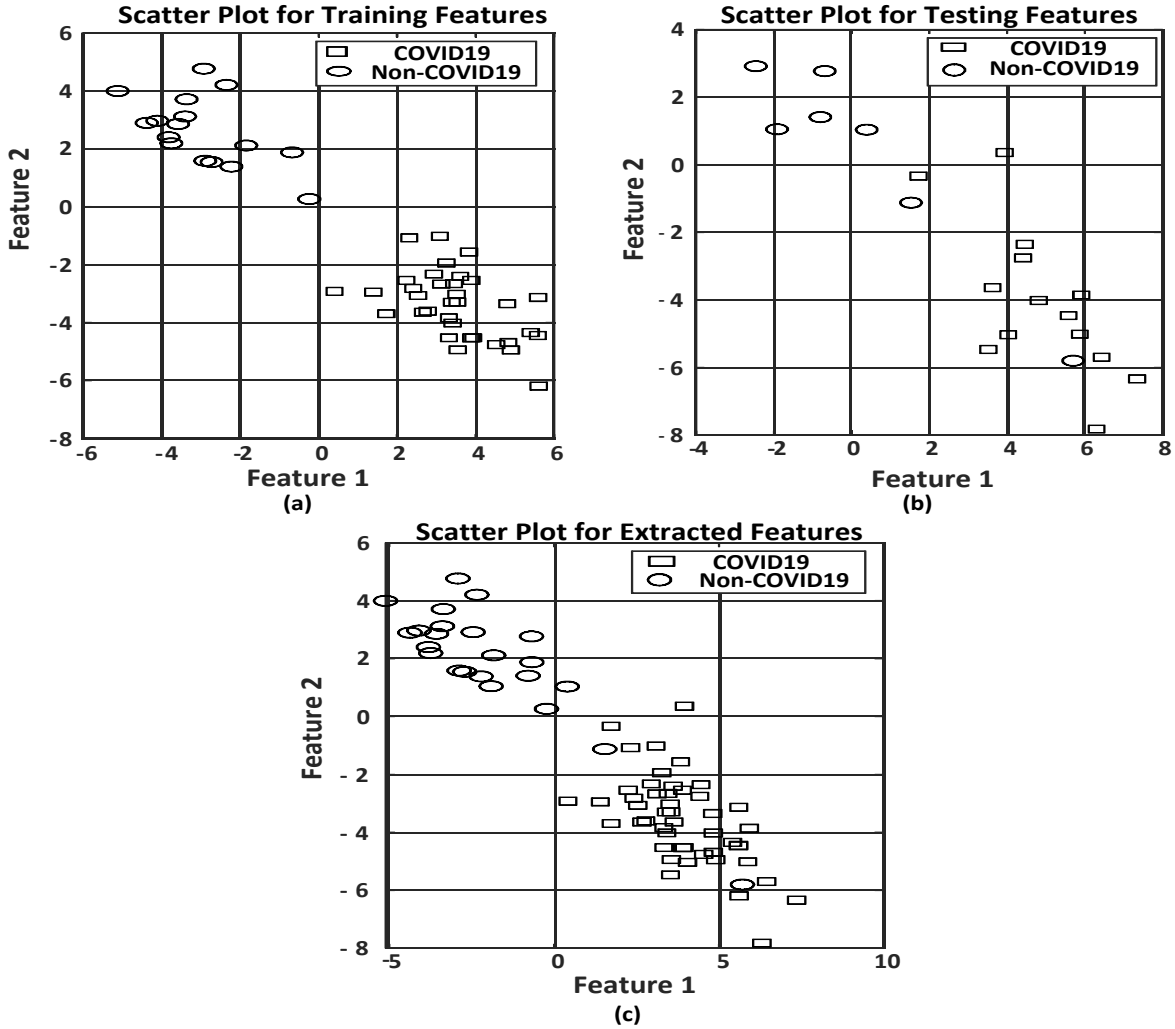

Fig. 4. The scatter distribution of two distinguished extracted features: a) from training set; b) from testing set; c) from both the training and the testing sets.

2.4. Classification Using SVM

This module aims to use SVM as a classifier rather than the Softmax classifier. The input to this module is the extracted deep features using CNN and the output is the corresponding class of these features. SVM is the most common type of classifiers used in binary classification problems. Linear SVM is the simplest form among all SVM types, and it is used when the data can be separated linearly, but if the number of features is more than two then the data can be separated using a hyperplane. The corresponding equation that describes the linear form is:

$$f(x) = \boldsymbol{w^T}.x + \mathrm{b} \tag{1}$$

where $f(x)$ is the class (it is either 1 or -1) , $\boldsymbol{w^T}$ is a normal vector to the hyperplane, x is the training data, and b is the bias.

If the data cannot be separated linearly, then another technique can be applied by mapping the input features into higher dimensional features to determine the separating hyperplane. This type of mapping function is called the kernel. There are different types of kernels: quadratic, polynomial and radial basis functions [15]. The kernel that has been employed in this investigation is the Gaussian radial basis function (RBF), which is given by the following equation with $\sigma > 0$ that defines the kernel width [16]:

$$K(x, y) = \exp(-\frac{\|x-y\|}{2\sigma^2}) \quad (2)$$

where $K(x, y)$ is the kernel function, x is the training data, y is the classes of training data, and σ is a factor that shapes the width of the radial basis function.

2.5. Classification Using RF

This module aims to use the RF as a classifier rather than the Softmax classifier. The input to this module are the deep features that are extracted using CNN and the output is the corresponding class of these features. RF algorithm was established by Breiman in 2001. It consists of a large number of individual decision trees that work collaboratively. Each distinct tree in this classifier develops a class prediction; and the class with the most elections is the model's prediction. The main advantage of RF is its simplicity and powerfulness. In data science-speak, RF works very well in many relatively uncorrelated models [17].

2.6. Performance Evaluation

The confusion matrix is the most commonly used indicator for evaluating the performance of the artificial intelligence algorithms (classifiers) [18]. It compares the output of the system with the reference data. The confusion matrix indicates the most common metrics, such as accuracy, sensitivity, specificity and precision. The accuracy indicates the ability of the classifier to differentiate between the classes correctly, while sensitivity refers to its ability to correctly detect the true positive. Specificity evaluates the actual negatives that are correctly identified by the classifier, while precision indicates the ability to predict true positive from all positives [16, 17]. Four statistical indices are calculated, namely, true positive (TP), false positive (FP), false negative (FN) and true negative (TN) in order to evaluate each of the aforementioned metrics as follows:

$$Accuracy = \frac{TP+TN}{TP+FP+TN+FN} \quad (3)$$

$$Sensitivity = \frac{TP}{TP+FN} \quad (4)$$

$$Precision = \frac{TP}{TP+FP} \quad (5)$$

$$Specificity = \frac{TN}{TN+FP} \quad (6)$$

A receiver operating characteristic curve (ROC) is a graphical plot that illustrates the diagnostic ability of a classifier model. It has two parameters: true positive rate (TPR) and false positive rate (FPR). Each parameter is computed as following [19, 20]:

$$TRP = \frac{TP}{TP+FN} \quad (7)$$

$$FPR = \frac{FP}{FP+TN} \quad (8)$$

ROC shows TPR versus FPR at various classification thresholds. The lowest parameter value indicates that the classifier can discriminate more subjects, which means an increase in both false positives and true positives is obtained [18].

3. RESULTS AND DISCUSSION

The proposed methodology was applied on chest X-ray images dataset, where CNN is utilized in two scenarios, the first one is in classification the dataset into COVID-19 and Non-COVID-19. In the second scenario it is employed to extract graphical features for hybrid system implementation. These two features were extracted from the FC layer for each image. CNN was trained using adaptive moment learning rate (ADAM) solver after applying data augmentation to increase the size of the dataset and to avoid overfitting during the training stage of the CNN. Then, these features were fed into two types of classifiers; SVM and RF. The proposed methodology, using the CNN-based system for classification of chest X-ray images proved to be a successful one in classifying the grayscale images with high performance. Fig. 5 shows class activation mapping (CAM) for two cases: COVID-19 and Non-COVID-19 using the last ReLU layer of the AOCT-Net. CAM is a method that is used to visualize where CNN is looking and what grasp CNN's attention in the input image for extracting the deep features. Using Fig. 5, we notice that CNN architecture pays attention to the regions of interest, where the COVID-19 affects the lungs (shown as a white spread area).

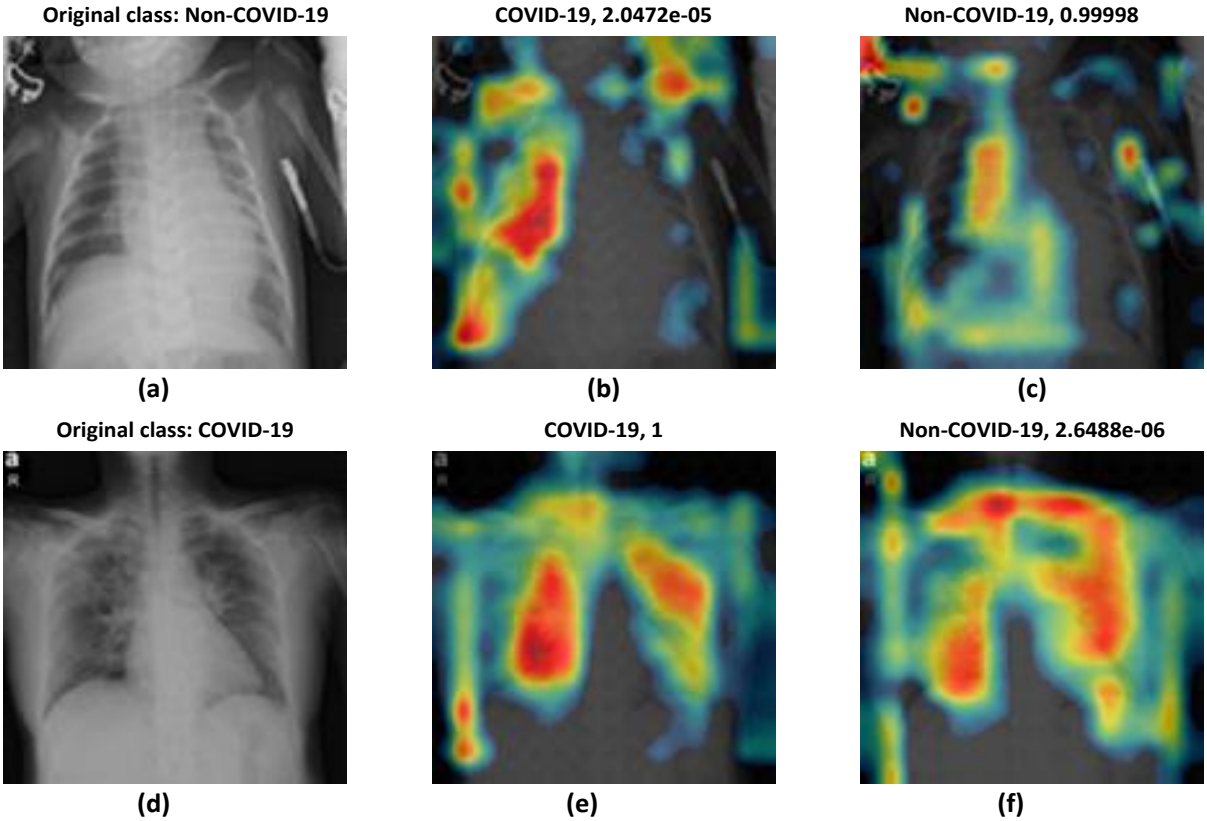

Fig. 5. Class activation mapping for COVID-19 and Non-COVID-19 pneumonia: a) input image of Non-COVID-19 class; b) COVID-19 features using CAM; c) Non-COVID-19 features using CAM; d) input image of COVID-19 class; e) COVID-19 features using CAM; f) Non-COVID-19 features using CAM.

The training and testing confusion matrices for all the employed classifiers are shown in Fig. 6. In addition, Table 1 shows a comparison between all the performance evaluation metrics for the used classifiers in the training stage and Table 2 represents the performance evaluation for the test stage for all the utilized classifiers. Table 3 exhibits the computation time for each of the utilized systems.

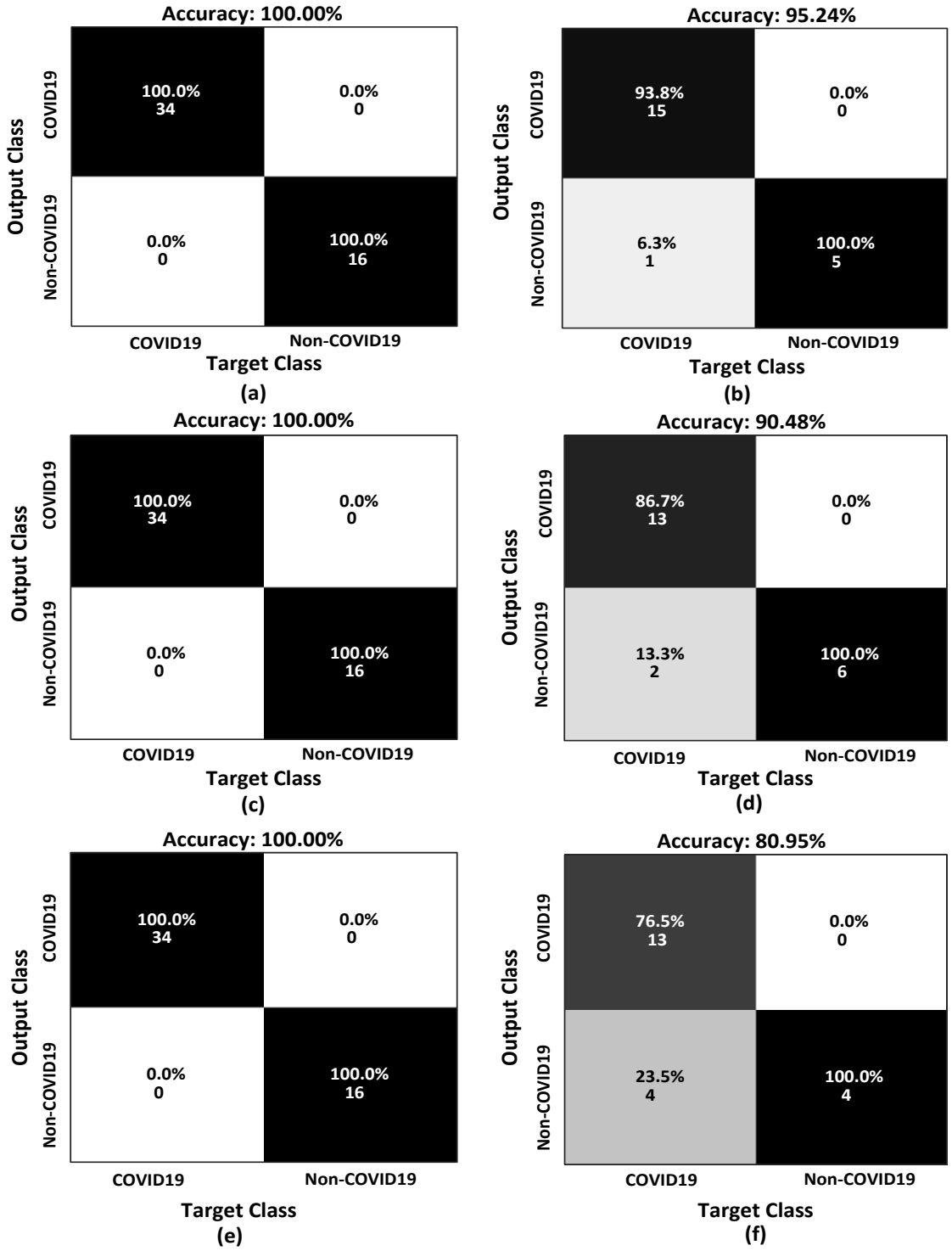

Fig. 6. Testing confusion matrices: a) CNN-Softmax Training; b) CNN-Softmax test; c) CNN-SVM training; d) CNN-SVM test; e) CNN-RF training; f) CNN-RF test.

Table 1. Training performance evaluation of classifiers.

Classifier	Accuracy [%]	Sensitivity [%]	Specificity [%]	Precision [%]
CNN-Softmax	100	100	100	100
CNN-SVM	100	100	100	100
CNN-RF	100	100	100	100

Table 2. Performance evaluation of classifiers in the test stage.

Classifier	Accuracy [%]	Sensitivity [%]	Specificity [%]	Precision [%]
CNN-Softmax	95.2	93.3	100	100
CNN-SVM	90.5	86.7	100	100
CNN-RF	81	76.5	100	100

Table 3. Testing time for each classifier.

Classifier	Time [s]
AOCT-Net	0.299704
SVM	0.168938
RF	0.551982

The used CNN has 95.2% accuracy, but the hybrid system with its features being extracted from the FC layer in the CNN exhibited 90.5% using the SVM classifier and 81% using the RF classifier. The performance of all classifiers in the training stage was 100%, but in the test stage, deep learning classification using the CNN classifier achieved better performance than the hybrid system. For the hybrid system, SVM obtained better results than RF due to RBF method. RF performance was the lowest among all classifiers because of the built trees that are combined with the majority voting technique for each input vector, in addition to the RF which is constructed using different base learners, and for each base learner an independent binary tree adopting recursive partitioning has been built.

Fig. 7 displays the error in classification training as a function of the used number of trees. It can be noticed that an increase in the number of trees leads to a decrease in the error of classification. Fig. 8 shows the decision tree base rule used for deciding where the input feature corresponded to class one (COVID-19) or class two (Non-COVID-19).

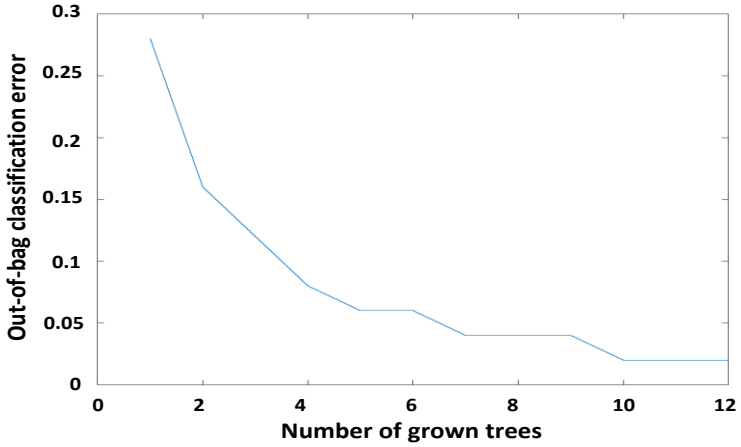

Fig. 7. Error variation over the number of used trees.

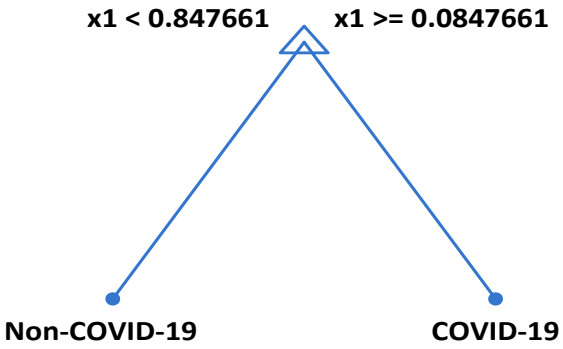

Fig. 8. The built RF model for classification.

4. CONCLUSIONS

In this paper, we utilized artificial intelligence techniques, namely, deep learning (CNN using Softmax classifier) and machine learning (SVM and RF) in building detection models that can discriminate between COVID-19 and Non-COVID-19 from chest X-ray images. The time consumption, as shown in Table 3, is less in SVM classifier than other classifiers. The results can be improved by obtaining a huge dataset of chest X-ray images in addition to building a model that uses CT images. In the future, we can use various types of classifiers besides different types of features such as local binary pattern (LBP) and texture features to describe the texture of the chest.

REFERENCES

[1] S. Stoecklin, P. Rolland, Y. Silue, A. Mailles, C. Campese, A. Simondon, M. Mechain, L. Meurice, M. Nguyen, C. Bassi, E. Yamani, "First cases of coronavirus disease 2019 (COVID-19) in France: surveillance, investigations and control measures, January 2020," *Eurosurveillance*, vol. 25, no. 6, pp. 2000094, 2020.

[2] Y. Jin, L. Cai, Z. Cheng, H. Cheng, T. Deng, Y. Fan, C. Fang, D. Huang, L. Huang, Q. Huang, Y. Han, "A rapid advice guideline for the diagnosis and treatment of 2019 novel coronavirus (2019-nCoV) infected pneumonia (standard version)," *Military Medical Research*, vol. 7, no. 1, pp. 4, 2020.

[3] F. Pan, T. Ye, P. Sun, S. Gui, B. Liang, L. Li, D. Zheng, J. Wang, R. Hesketh, L. Yang, C. Zheng, "Time course of lung changes on chest CT during recovery from 2019 novel coronavirus (COVID-19) pneumonia," *Radiology*, pp. 200370, 2020.

[4] F. Rabi, M. Al Zoubi, G. Kasasbeh, D. Salameh, A. Al-Nasser, "SARS-CoV-2 and coronavirus disease 2019: what we know so far," *Pathogens*, vol. 9, no .3, pp. 231, 2020.

[5] X. Xu, X. Jiang, C. Ma, P. Du, X. Li, S. Lv, L. Yu, Y. Chen, J. Su, G. Lang, Y. Li, "Deep learning system to screen coronavirus disease 2019 pneumonia," *ArXiv Preprint ArXiv:2002.09334*, 2020.

[6] S. Wang, B. Kang, J. Ma, X. Zeng, M. Xiao, J. Gu, M. Cai, J. Yang, Y. Li, X. Meng, B. Xu, "A deep learning algorithm using CT images to screen for Corona Virus Disease (COVID-19)," *MedRxiv*, pp. 3-19, 2020.

[7] A. Hamed, "Image processing of corona virus using interferometry," *Optics and Photonics Journal*, vol. 6, no. 5, pp. 75, 2016.

[8] J. Cohen, P. Morrison, L. Dao, "COVID-19 Image data collection," *ArXiv:2003.11597*, 2020. <https://github.com/ieee8023/covid-chestxray-dataset>

[9] J. Cohen, "COVID-19 image data collection," ArXiv Preprint ArXiv:2003.11597, 2020.

[10] A. Alqudah, S. Qazan, "Augmented COVID-19 X-ray images dataset," *Mendeley Data, V4, 2020.* <http://dx.doi.org/10.17632/2fxz4px6d8.4>

[11] C. Shorten, T. Khoshgoftaar, "A survey on image data augmentation for deep learning," *Journal of Big Data*, vol. 6, no. 1, pp. 60, 2019.

[12] M. Żejmo, M. Kowal, J. Korbicz, R. Monczak, "Classification of breast cancer cytological specimen using convolutional neural network," *Journal of Physics: Conference Series*, vol. 783, no. 1, pp. 012060, 2017.

[13] F. Spanhol, L. Oliveira, C. Petitjean, L. Heutte, "Breast cancer histopathological image classification using convolutional neural networks," 2016 International Joint Conference on Neural Networks, Vancouver, BC, pp. 2560-2567, 2016.

[14] A. Alqudah, "AOCT-NET: a convolutional network automated classification of multiclass retinal diseases using spectral-domain optical coherence tomography images," *Medical and Biological Engineering and Computing*, vol. 58, no. 1, pp. 41-53, 2020.

[15] M. Nanda, K. Seminar, D. Nandika, A. Maddu, "A comparison study of kernel functions in the support vector machine and its application for termite detection," *Information*, vol. 9, no. 1, pp. 5, 2018.

[16] D. Bowes, H. Tracy, D. Gray, "Comparing the performance of fault prediction models which report multiple performance measures: recomputing the confusion matrix," *Proceedings of the 8th International Conference on Predictive Models in Software Engineering*, pp. 109-118, 2012.

[17] A. Alqudah, H. Alquraan, I. Abu-Qasmieh, A. Al-Badarneh, "Employing image processing techniques and artificial intelligence for automated eye diagnosis using digital eye fundus images," *Journal of Biomimetics, Biomaterials and Biomedical Engineering*, vol. 39, pp. 40-56, 2018.

[18] A. Alqudah, "Towards classifying non-segmented heart sound records using instantaneous frequency based features," *Journal of Medical Engineering and Technology*, vol. 43, no. 7, pp. 418-430, 2019.

[19] D. Hand, R. Till. "A simple generalisation of the area under the ROC curve for multiple class classification problems," *Machine Learning*, vol. 45, no. 2, pp. 171-186, 2001.

[20] A. Alqudah, S. Qazan , A. Alqudah, "Automated systems for detection of COVID-19 using chest X-ray images and lightweight convolutional neural networks," *Europe PMC*, 2020.